Supporting materials:

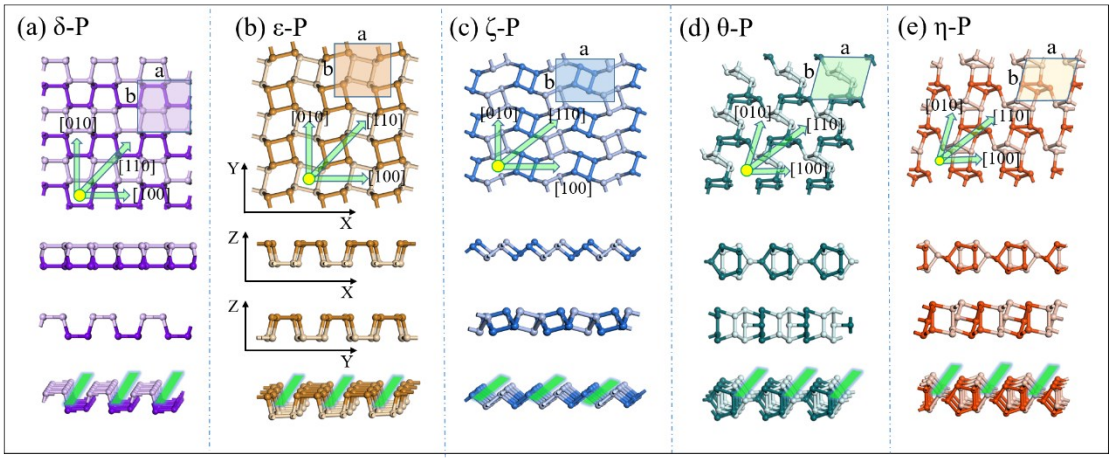

Fig. S1 Graphic structures of the other four phosphorus monolayers (a) δ-P, (b) ε-P, (c) ζ-P, (d) θ-P, (e) η-P. Top views, side views, and the most convenient diffusion grooves in phosphorene polymorphs.

Table S1 Lattice parameters of phosphorus monolayers. Planar atomic density is defined as the atom number in the monolayer per square angstrom ($\rho = \frac{N}{S}$, N denotes the atom number in the same plane of the cell unit and S represents the area of the cell unit.). Relative stability of the monolayer polymorphs is assessed based on $\Delta E = E - E(\alpha\text{-}P)$, the energy difference relative to α-P.

Items	δ-P		ε-P		ζ-P		θ-P		η-P	
	This work	Cal.	This work	Cal.	This work	Cal.	This work	Cal.	This work	Cal.
a/Å	5.55	5.56[29]	5.32	5.37[26]	6.40	6.43[26]	6.18	6.22[26]	6.32	6.32[26]
b/Å	5.46	5.46[29]	5.32	5.37[26]	5.25	5.32[26]	5.56	5.50[26]	5.4	5.40[26]
α/°	90	90[29]	90		90		90	90[26]	90	90[26]
β/°	90	90[29]	90		138		90	90[26]	90	90[26]
γ/°	90	90[29]	90	90[26]	90	90[26]	76.5	76.8[26]	77.14	77.16[26]
Unit	3*3		3*3		3*3		3*3		3*3	
ρ/(n/Å^2)	0.264		0.267		0.231		0.301		0.296	
ΔE (eV/atom)	0.07	0.07[29]	0.15	0.13[26]	0.10	0.10[26]	0.02	0.01[26]	0.05	0.05[26]

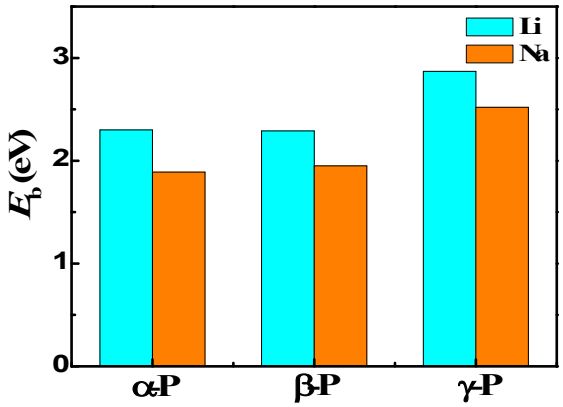

Fig. S2 Adsorption energies of Li/Na atoms on α-P, β-P and γ-P.

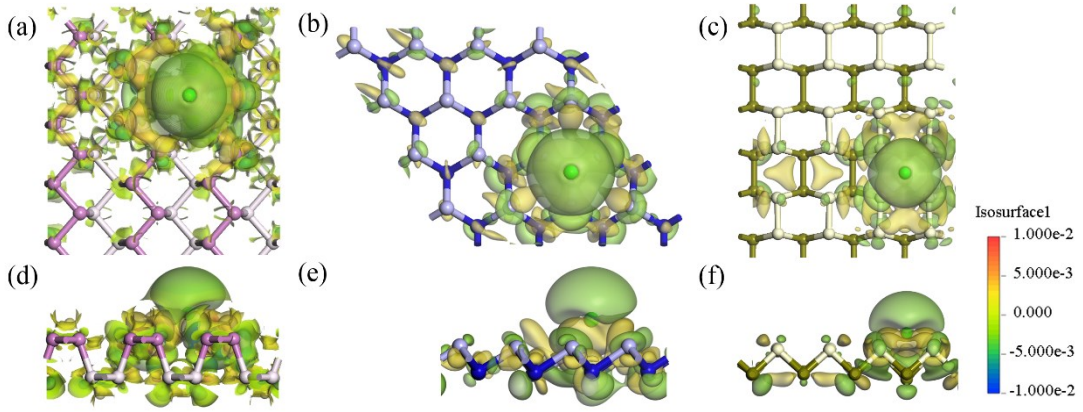

Fig. S3 The electron density difference between before and after Li adsorbed states. The charge transfer is defined as the charge difference between with and without absorbed Na ion, and can be expressed as $\Delta\rho = \rho(P + Li) - \rho(P) - \rho(Li)$, where $\rho(P + Li)$, $\rho(P)$ and $\rho(Na)$ are the charge densities for bound system, pristine Phosphorus substrate and Na atom, respectively. Here, green (yellow) is the spatial regions gain (loss) in charge. The isosurface level is set as 0.003 e Å^{-3}. Top views (a) α-P with Li, (b) β-P with Li, (c) γ-P with Li, side views (d) α-P with Li, (e) β-P with Li, (f) γ-P with Li.

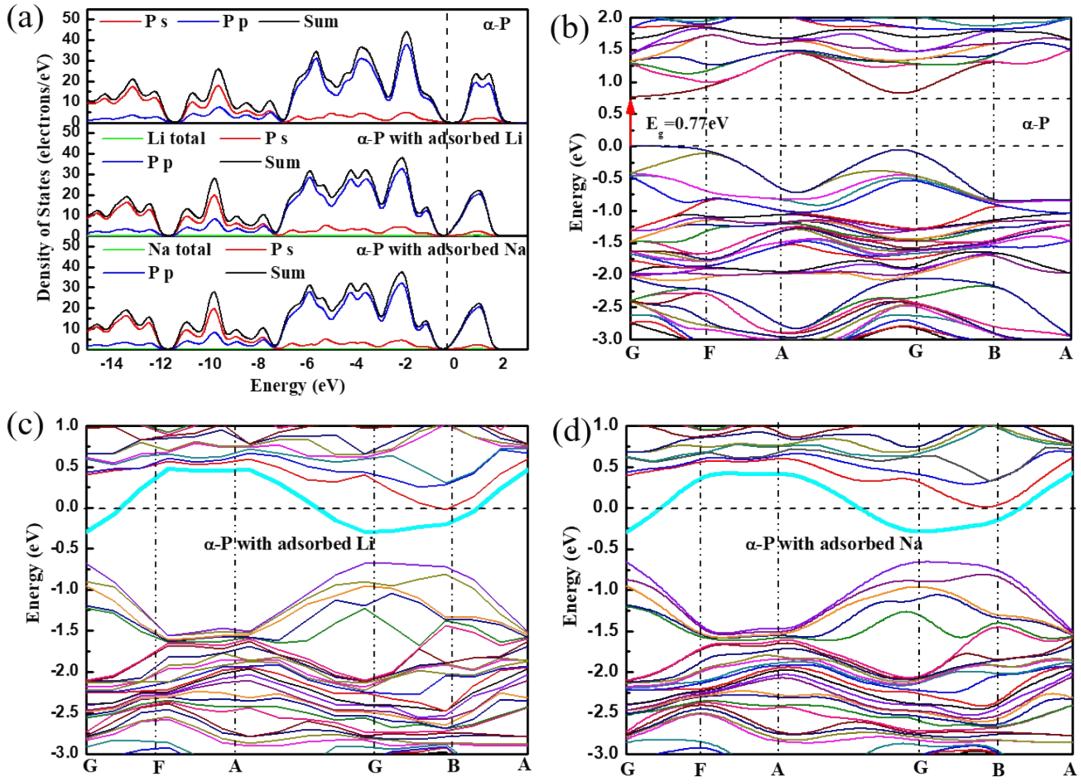

Fig. S4 (a) Atomic partial density of states (PDOS) for pristine α-P and α-P with adsorbed Li or Na; (b) Band structure of pristine α-P; (c) Band structure of α-P with adsorbed Li; (d) Band structure of α-P with adsorbed Na.

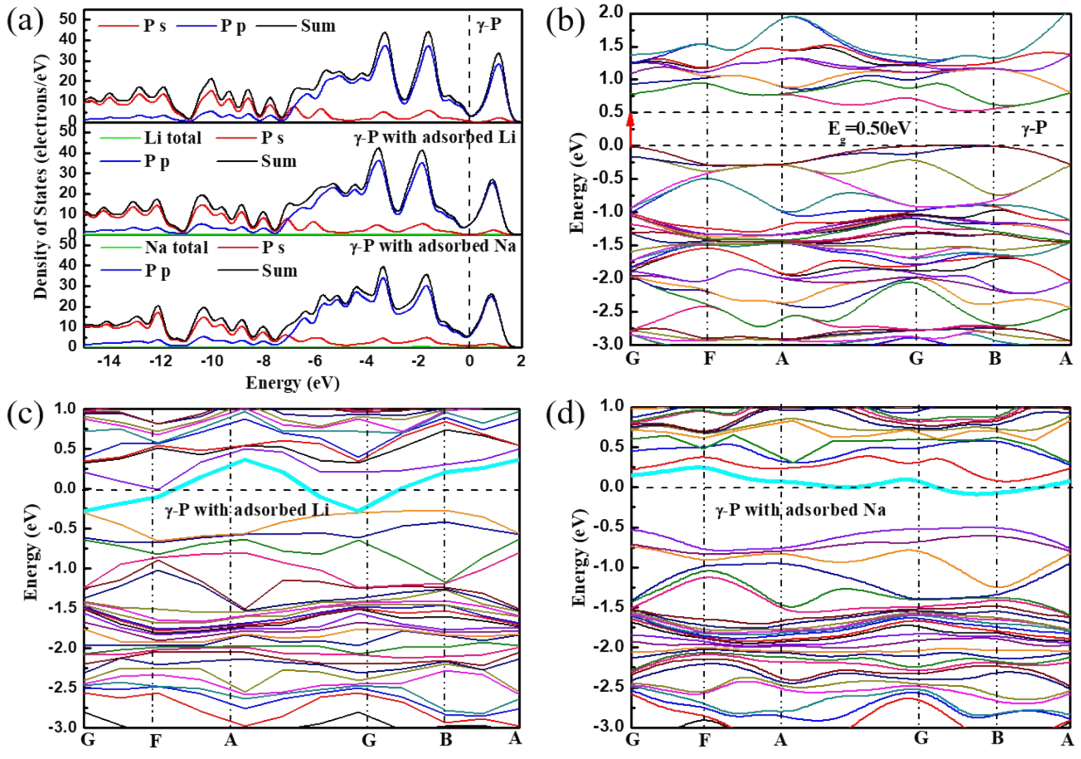

Fig. S5 (a) Atomic partial density of states (PDOS) for pristine γ-P and γ-P with adsorbed Li or Na;

(b) Band structure of pristine γ-P; (c) Band structure of γ-P with adsorbed Li; (d) Band structure of γ-P with adsorbed Na.

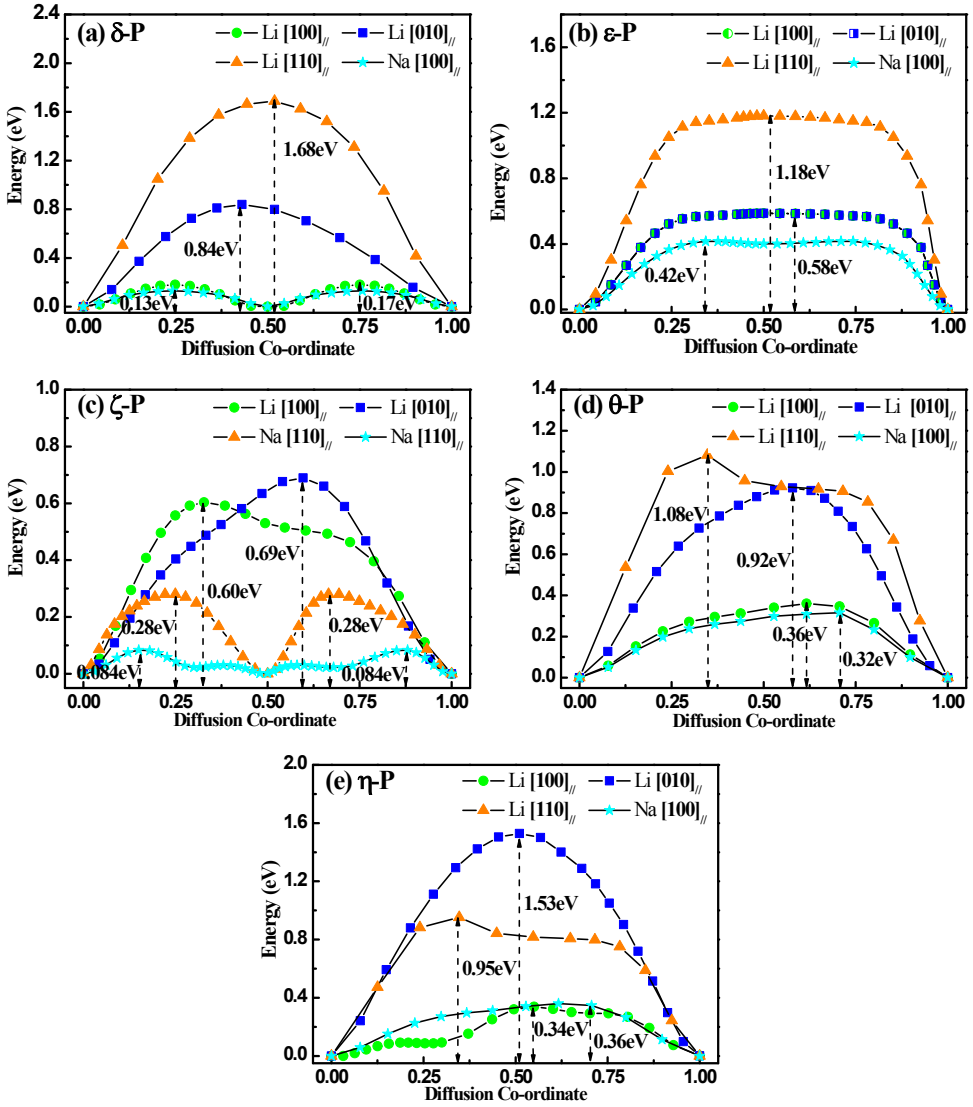

Fig. S6 Energy profiles of Li/Na diffusion along the grooves of phosphorene polymorphs. (a) Li/Na diffusion on δ-P, (b) Li/Na diffusion on ε-P, (c) Li/Na diffusion on ζ-P, (d) Li/Na diffusion on θ-P, (e) Li/Na diffusion on η-P. Diffusion directions of Li/Na diffusion are shown in Fig. S1 with the most fluent diffusion grooves shown at the bottom of Fig. S1.

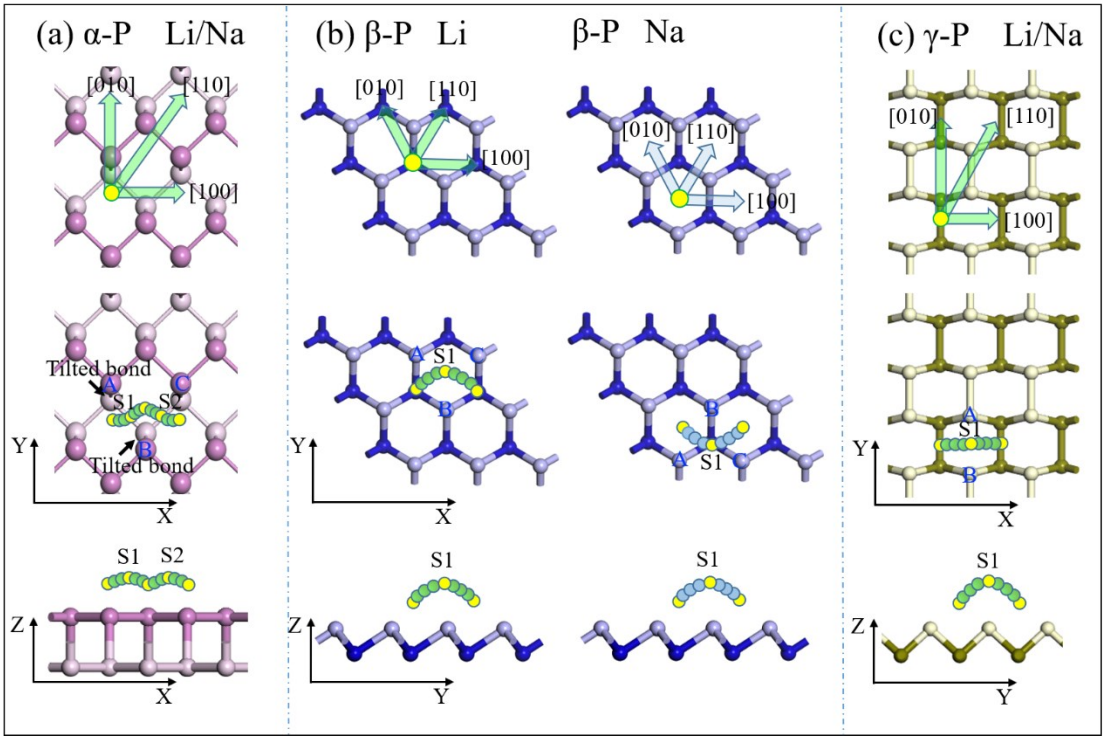

Fig. S7 Diffusion trajectories of Li atom on different phosphorus polymorphs (S1 and S2 denote the barrier points along the most convenient diffusion path). (a) α-P, (b) β-P, (c) γ-P. Diffusion directions, top view and side view of Li diffusion pathways along the [100] direction.

In this work, we consider a series of configurations with various stoichiometry proportions of Li_xP and Na_xP (x = 0.042, 0.056, 0.083, 0.125, 0.25, 0.5 and 1 for α-P, x = 0.04, 0.0625, 0.167, 0.25, 0.333, 0.5 and 1 for β-P, and x = 0.042, 0.083, 0.125, 0.25, 0.5 and 1 for γ-P), as shown in Figs. S7-S9 with two Li/Na atoms absorbed on upper and lower surfaces of phosphorene anodes, with the computational units in 4×3 (Li_2/Na_2P_{48}), 3×3 (Li_2/Na_2P_{36}), 3×2 (Li_2/Na_2P_{24}), 2×2 (Li_2/Na_2P_{16}), 2×1 (Li_2/Na_2P_8), 1×1(Li_2/Na_2P_4) and 1×1(Li_4/Na_4P_4) for α-P, 5×5 (Li_2/Na_2P_{50}), 4×4 (Li_2/Na_2P_{32}), 3×3 (Li_2/Na_2P_{18}), 2×2 (Li_2/Na_2P_8), 3×1 (Li_2/Na_2P_6) and 1×1(Li_2/Na_2P_2) for β-P, and 4×3 (Li_2/Na_2P_{48}), 3×2 (Li_2/Na_2P_{24}), 2×2 (Li_2/Na_2P_{16}), 2×1 (Li_2/Na_2P_8), 1×1(Li_2/Na_2P_4) and 1×1 (Li_4/Na_4P_4) for γ-P, respectively. The adatoms were placed over the most stable sites of phosphorene substrates at 3 Å above the substrate for double-sided adsorption, and keep the adsorbed atoms separated as far as possible. We also calculated the corresponding models by adsorbing two atoms at the same side of the phosphorene. The results show that all the models with two atoms adsorbed at both sides of phosphorene have lower energy. In order to determine the adsorption stability, the method proposed by Tritsaris et al. [1] was employed; wherein, after removing the adsorbed atoms, a new geometry optimization was carried out on the bare distorted substrate. For Li/Na adsorption on these three phosphorene anodes, the structural parameters of the final system (such as lattice constant, bond length and bond angles) were very similar to the original phosphorene, indicating that the matrix underwent reversible deformation during the adsorption process.

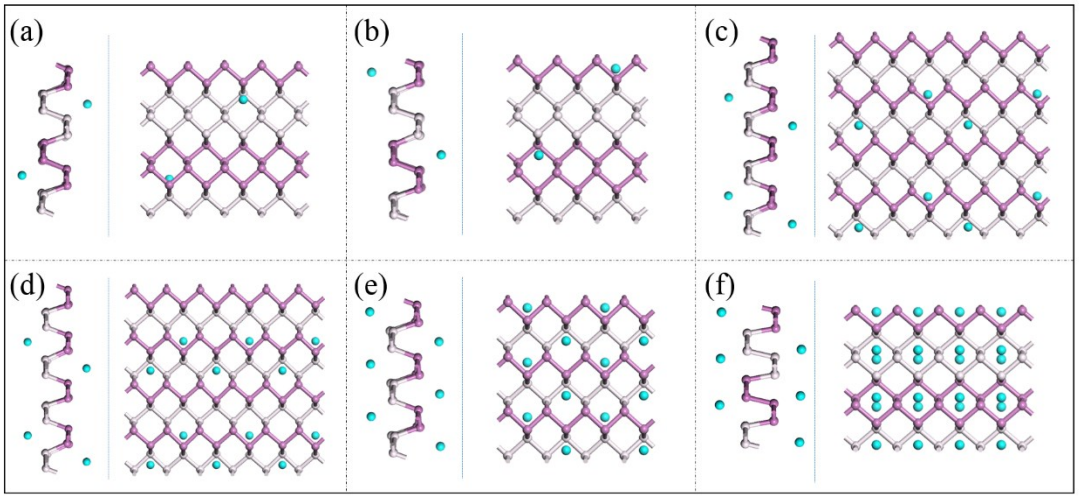

Fig. S8 Calculation configurations of α-P with various stoichiometry proportions in Li_xP/Na_xP. (a) x = 0.042, (b) x = 0.056, (c) x =0.083, (d) x =0.125, (e) x =0.25, (f) x =0.5, with two Li/Na atoms absorbed on upper and lower surfaces of α-P. Cyan spheres represent adsorbed Li/Na atoms, and other colors show P atoms located in different layers.

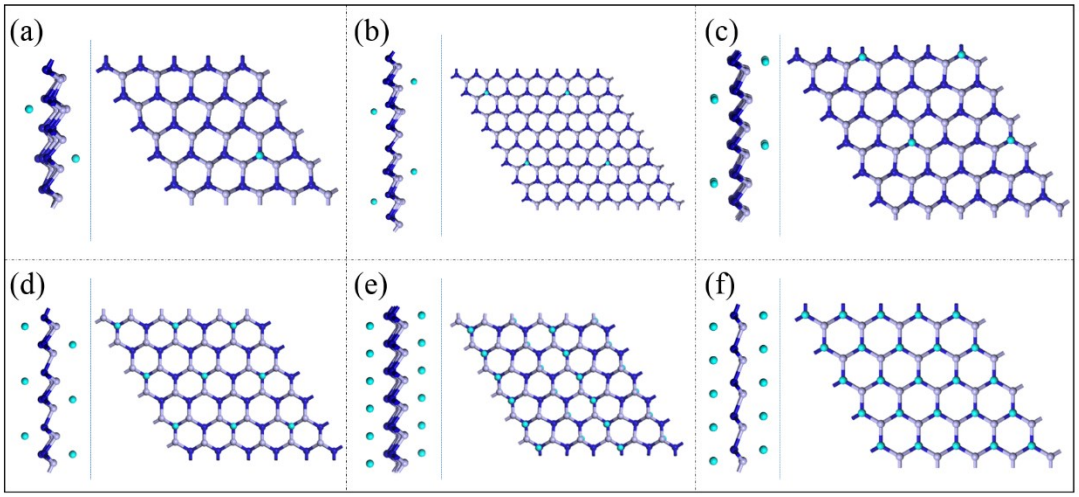

Fig. S9 Calculation configurations of β-P with various stoichiometry proportions in Li_xP/Na_xP. (a) x = 0.04, (b) x = 0.0625, (c) x = 0.167, (d) x = 0.25, (e) x = 0.5 and (f) x = 1, with two Li/Na atoms absorbed on upper and lower surfaces of β-P. Cyan spheres represent adsorbed Li/Na atoms, and other colors show P atoms located in different layers.

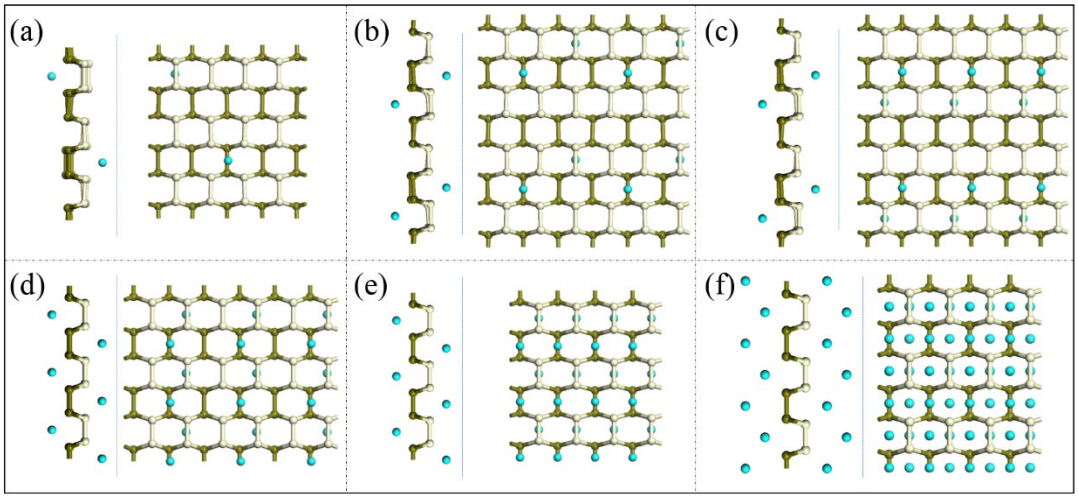

Fig. S10 Calculation configurations of γ-P with various stoichiometry proportions in Li_xP/Na_xP. (a) $x = 0.042$, (b) $x = 0.083$, (c) $x = 0.125$, (d) $x = 0.25$, (e) $x = 0.5$ and (f) $x = 1$, with two Li/Na atoms absorbed on upper and lower surfaces of γ-P. Cyan spheres represent adsorbed Li/Na atoms, and other colors show P atoms located in different layers.

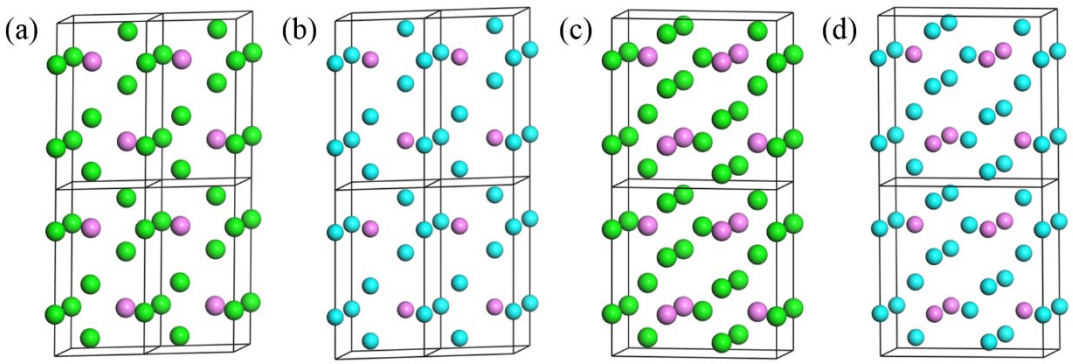

Fig. S11 Crystal structures of final products Li_3P/Na_3P at the full lithiation/sodiation state. (a) Li_3P and (b) Na_3P in primitive cells with hexagonal lattice type, (c) Li_3P and (d) Na_3P in redefined supercell with orthorhombic lattice type.

Table S2 Lattice parameters of final products Li_3P/Na_3P at the full lithiation/sodiation states, and lattice parameters of phosphorene α-P, β-P and γ-P with corresponding theoretical expansion rates.

Items	Li_3P	β-P	Li_3P	α-P	γ-P
Lattice type	hexagonal	hexagonal	orthorhombic	orthorhombic	orthorhombic
a/Å	3.83	3.29	3.83	3.30	3.40
Expansion rate		16.4%		16%	12.6%
b/Å	3.83	3.29	6.63	4.56	5.35
Expansion rate		16.4%		45.4%	23.9%
c/Å	6.71		6.71		
α/°	90	90	90	90	90
β/°	90	90	90	90	90

γ/°	120	120	90	90	90

Items	Na_3P	β-P	Na_3P	α-P	γ-P
Lattice type	hexagonal	hexagonal	orthorhombic	orthorhombic	orthorhombic
a/Å	4.46	3.29	4.46	3.30	3.40
Expansion rate		35.5%		35.1%	31.1%
b/Å	4.46	3.29	7.72	4.56	5.35
Expansion rate		35.5%		69.3%	44.4%
c/Å	7.73		7.73		
α/°	90	90	90	90	90
β/°	90	90	90	90	90
γ/°	120	120	90	90	90

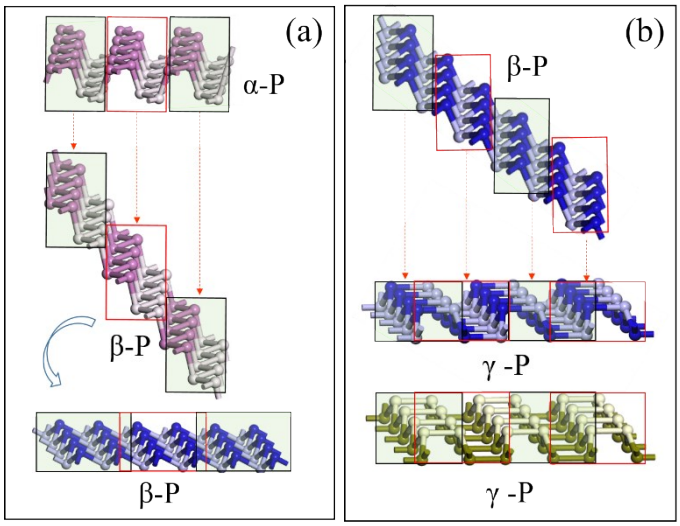

Fig. S12 Schematic diagrams of the conversions by embedding an array of dislocations, with the corresponding structural units highlighted by shaded regions and arrows. (a) from α-P to β-P, (b) from β-P to γ-P.

References:

[1] G. A. Tritsaris, E. Kaxiras, S. Meng and E. Wang, 2013, *Nano Lett*, 13 (5): 2258-2263.